Structural Response of a Highly Viscous Aluminoborosilicate Melt to Isotropic and Anisotropic Compression

ARTICLE *in* THE JOURNAL OF CHEMICAL PHYSICS · SEPTEMBER 2009

Impact Factor: 2.95 · DOI: 10.1063/1.3223282

7 AUTHORS, INCLUDING:

Jingshi Wu
Corning Incorporated
10 PUBLICATIONS **144** CITATIONS
SEE PROFILE

Harald Behrens
Leibniz Universität Hannover
93 PUBLICATIONS **2,460** CITATIONS
SEE PROFILE

Lothar Wondraczek
Friedrich Schiller University Jena
184 PUBLICATIONS **2,262** CITATIONS
SEE PROFILE

Yuanzheng Yue
Aalborg University
201 PUBLICATIONS **2,651** CITATIONS
SEE PROFILE

Structural response of a highly viscous aluminoborosilicate melt to isotropic and anisotropic compressions

Jingshi Wu,[1] Joachim Deubener,[2,a)] Jonathan F. Stebbins,[1] Lenka Grygarova,[2] Harald Behrens,[3] Lothar Wondraczek,[4] and Yuanzheng Yue[5]
[1]*Department of Geological and Environmental Sciences, Stanford University, Stanford, California 94305, USA*
[2]*Institute of Non-Metallic Materials, Clausthal University of Technology, 38678 Clausthal-Zellerfeld, Germany*
[3]*Institute of Mineralogy, Leibniz University Hannover, 30167 Hannover, Germany*
[4]*Department of Materials Science, Friedrich-Alexander-University, Erlangen-Nürnberg, 91058 Erlangen, Germany*
[5]*Section of Chemistry, Aalborg University, 9000 Aalborg, Denmark*

(Received 21 June 2009; accepted 14 August 2009; published online 10 September 2009)

Aluminoborosilicate melts of E-glass composition have been compressed at pressures up to 500 MPa and subsequently cooled (4–5 K min^{-1}) under pressure from well above the glass transition to room temperature. It is found that increasing uniaxial pressure lead to anisotropic glasses with increasing permanent birefringence, while increasing isostatic pressure resulted in isotropic glasses with increasing density (compaction of 2.1% at 500 MPa). Static and magic-angle spinning nuclear magnetic resonance spectroscopy of ^{11}B, ^{23}Na, ^{27}Al, and ^{29}Si were performed to explore pressure-induced changes in the short-range structure of these glasses. NMR experiments readily detected increasing ^{IV}B, ^{V}Al, and ^{VI}Al concentrations with pressure as well as a decrease in the mean distance of sodium to oxygen atoms (0.7% at 500 MPa), but no detectible evidence of short-range structural orientation around these atoms in the birefringent glasses were found. Quantifying the changes in the local boron, aluminum, silicon, and sodium environments revealed that the measured increase of recovered density with pressure in E-glass can only be partly explained by increase in B and Al coordination, and that overall compression of the network and of the network modifier cation volumes must also be important. Structural changes in the intermediate range, which were not detected by NMR, are discussed as a source of birefringence in anisotropic E-glass. © *2009 American Institute of Physics*. [doi:10.1063/1.3223282]

I. INTRODUCTION

Inter-relation between structure and macroscopic properties of glasses is of particular interest if anisotropy is observed. Anisotropy of glass has been considered as a consequence of the liquidlike behavior in the melt, retaining, however, a considerable degree of local molecular ordering based on persistent nonisometric units (e.g., chain fragments).[1,2] A general feature of these melts is the relative ease of obtaining flow-induced orientation effects, which have been considered therefore as sensors of the structural properties.[3] Anisotropy can be induced in the flowing liquid by applying a defined shear or strain rate and subsequently frozen into the glass by cooling below the glass transition. If reannealed in the absence of external constraints, recovery of the isotropic state occurs exothermically.[4] Several anisotropic effects have been observed in glasses after such thermomechanical treatments, primarily either optical (birefringence, specific birefringence) or mechanical (strain, Poisson ratio), see, e.g., review in Ref. 5. Anisotropic properties have been found to be readily inducible in phosphate, borate, and silicate liquids of wide compositional ranges.[6] They increase with decreasing structural connectivity, yielding maximum values in linearly branched metaphosphate liquids at 10^5 Pa s.[5] However, short-range structural changes related to anisotropy have been observed only in a few glass systems. These include extruded rods and birefringent fibers of metaphosphate compositions formed at extreme strain rates, which result in orientation-dependent static ^{31}P nuclear magnetic resonance spectroscopy (NMR) spectra,[7,8] and nonisometric halos of wide angle x-ray diffraction (WAXS) patterns.[9] In contrast to the behavior of the "polymerlike" structure of metaphosphate glasses, the lack of short-range structural orientation in birefringent borosilicate, boron oxide and silicate glass fibers has been evidenced by ^{11}B, ^{27}Al, and ^{29}Si NMR (Ref. 10) as well as by WAXS.[9] However, as most of these investigations have been conducted in glass fibers, results, in particular, on local boron environment, could be influenced by thermal histories (described by high fictive temperature T_f) due to hyperquenching and, thus, do not allow final conclusions on the quantification of structural anisotropy.

Among the network cations (e.g., B^{3+}, Al^{3+}, Si^{4+}, and P^{5+}) dominating the short-range structure of most industrially produced multicomponent oxide glasses, boron is unique in readily transforming between three (^{III}B) and four (^{IV}B) coordination (herein expressed as N_4=the ratio of tetrahedral to

a)Electronic mail: joachim.deubener@tu-clausthal.de.

total boron) with changes in composition, temperature, and pressure. The compositional effect, termed the "boron anomaly" by glass technologists, provides the basis for widely used borosilicate glasses of low thermal expansion produced by industry over the several past decades, *inter alia* as E-glass fibers for reinforcing composite materials.

Changes in the relative abundances of ^{III}B and ^{IV}B in borate, borosilicate, and multicomponent boron-bearing glasses formed with varying temperature and pressure history have been observed, using ^{11}B NMR as a nucleus-specific technique sensitive to the local bonding of boron atoms in glasses. The experiments have demonstrated an increase in N_4 with both decreasing T_f (Refs. 11–14) and increasing fictive pressure p_f.[15–17] It has been shown that, with respect to N_4, equivalent glasses can be generated on both preparation paths, i.e., produced by compression or by different cooling rates.[17] However, it was also demonstrated that such glasses differ in density and excess enthalpy, which reflects decoupling of mechanical and caloric relaxation on different generation paths on the p-T landscape.[18]

A number of studies have applied NMR spectroscopy and other measurements to quantifying structural changes in oxide glasses quenched from above T_g at high pressure, as recently summarized.[16,19–24] Although there is evidence from *in situ* spectroscopy that some structural changes in compressed glasses can at least partially relax on decompression even at ambient temperature,[25] some of these reports describe changes in Al, B, Si, Na, and O coordination that are clearly correlated with measured, recovered densification of the glasses and thus must be closely related to the compaction mechanism.[21–24]

In this study, a commercial aluminoborosilicate glass (E-glass) was considered. Both isostatically and uniaxially compressed samples were produced at pressures up to 500 MPa, but, in contrast to the previously studied glass fibers,[10] cooled slowly (4–5 K min^{-1}) under pressure to room temperature in order to freeze in the structure of the compressed glass-forming liquid with standard thermal conditions, i.e., $T_f \approx T_g$. In this way we were able to link compaction and birefringence with changes in the short-range structure in samples with the same thermal history. Static and magic-angle spinning (MAS) ^{11}B NMR experiments were carried out to explore the increase of N_4 with pressure. Here we ask the question: Can the compaction of the glass be exclusively attributed to the changes in boron coordination? To answer this, ^{23}Na, ^{27}Al, and ^{29}Si NMR experiments have been conducted as well. By taking into account the extent of compression caused by changes in the local structure around Na, Al, and Si (coordination numbers, bond distances, and angles) and by comparing this value with changes in density, we have gathered information on possible contributions of larger structural ranges (midrange) on compaction and birefringence.

II. EXPERIMENTAL

A. Starting material and high-pressure experiments

The starting glass for all experiments was a sample of E-glass as described in a recent detailed study of the relaxation kinetics of fibers of this composition[26] (Table I). The batch was melted at 1773 K for 2 h in an electrical furnace using a Pt/Rh crucible, and subsequently poured onto a steel plate to form a disk of nearly 10 mm thickness and 100 mm diameter. The disk was cooled at 943 K for 1 h before the heater power was shut off, which resulted in a cooling rate of 5–7 K min^{-1} to room temperature. From the disk, cylinders, and rods were cored for uniaxial and isostatic compression experiments, respectively.

TABLE I. Composition of glasses compared in this study, in mol %.

	E-glass[a]	E-glass[b]	Na-borosilicate[c]	Na-borosilicate[d]
SiO_2	56.5	56.8	74	49.3
Al_2O_3	9.1	9.2	⋯	⋯
B_2O_3	5.7	8.1	10	24.6
MgO	⋯	7.0	⋯	⋯
CaO	26.5	18.9	⋯	⋯
Na_2O	0.9		16	26.1
Fe_2O_3	0.1		⋯	⋯
F_2	1.2		⋯	⋯

[a]This study.
[b]References 27 and 28.
[c]Reference 17.
[d]Reference 15.

Uniaxial compression experiments were carried out using an Instron 8562 testing machine at axial pressures up to 142 MPa. Glass cylinders (diameter=9.7 mm, height h_0 =7.3 mm) were compressed under constant pressure at the Isokom temperature $T_{11}=966\pm3$ K [Newtonian viscosity $=10^{11}$ Pa s (Ref. 29)] for 10 min and subsequently cooled under pressure at 5 K min^{-1} to room temperature. Newtonian flow is assumed to be active during loading at T_{11}. Non-Newtonian flow and therefore a deviation from the initial linear stress-birefringence correlation have been observed in silicate glasses of comparable connectivity at axial pressures >200 MPa.[6] The degree of axial compression $\Delta h/h_0$ was in the range from 16.7% to 28.6%. Complete elimination of thermal stresses after cooling in all cylindrical samples was confirmed by the fact that no birefringence was observed with the polarized light traveling parallel to the axial direction. Birefringence was observed only with the polarized light beam perpendicular to the axial cylinder and compression direction.

In accordance with previous studies,[17,18,30] isostatic compression experiments were performed at pressures of up to 500 MPa in a cold seal pressure vessel (CSPV). Individual rods ($4\times4\times25$ mm^3) were loaded directly into the CSPV and equilibrated under pressure at 983 ± 5 K for 10 min, i.e., well above the glass transition temperature T_g of 952 K (Ref. 26) and, thus, significantly longer than the relaxation time τ of ≈0.4 s.[29] Temperature was recorded continuously with a NiCr–Ni thermocouple in a bore hole at the end of the autoclave. Temperature at the sample position was calibrated under pressure in a separate run using three NiCr–Ni thermocouples (accuracy of ±5 K) that were inserted into the autoclave. Pressure was held constant with an automatic pumping system, and was measured by a strain gauge manometer (accuracy of ±5 MPa). Samples were cooled under

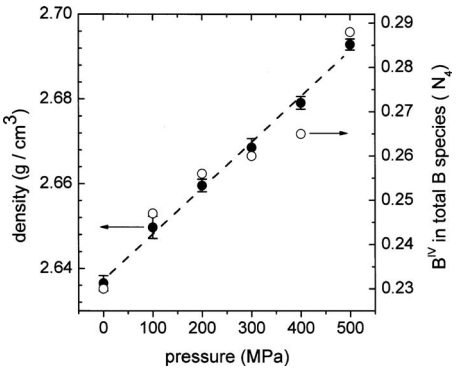

FIG. 1. Density and fraction of tetrahedrally coordinated boron (N_4) of isostatically compressed E-glass samples. The line indicates best linear fit through the density data.

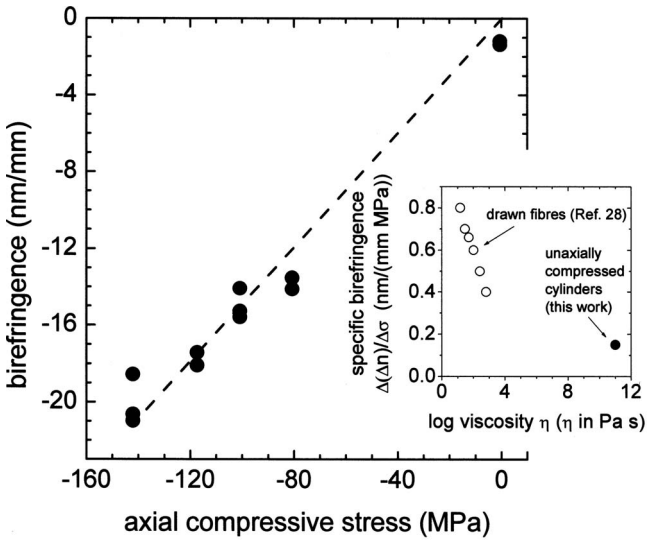

FIG. 2. Birefringence of uniaxially compressed E-glass samples. Line indicates best linear fit through the data. The inset shows the specific birefringence as a function of viscosity for different E-glasses. Fiber data (Ref. 28) (see Table I for composition).

pressure at $4.0-4.5\pm0.2$ K min^{-1} down to room temperature. After the high-pressure experiments, samples were checked by optical microscopy and powder x-ray diffraction (XRD) and no crystals were detected in the glasses. None of the NMR experiments suggested the presence of crystals.

B. Density measurements

The density of each sample was determined by helium pycnometry. Isostatically compressed samples were polished (silicon carbide and ethanol) on all sides, removing $\approx$150 μm of the surface to avoid any interference from surface alteration or diffusion: During compression, samples were in direct contact with the compression medium argon and atmospheric impurities that might diffuse into the glass.

C. Determination of birefringence

Polarized light microscopy (Olympus BX60) was used for the birefringence measurements. Uniaxially compressed cylinders were cut parallel to the cylinder axis to obtain a $\approx$3.5 mm thick platelet of the central section. Platelets were adjusted on the microscope stage to the 45°-position between crossed polarizers. The existence and orientation of optical anisotropy was verified using a quartz retardation plate (530 nm). Birefringence was measured at the center and along the equatorial line (at a radial distance of 2 mm from the center) of the platelet using a Berek compensator and monochromatic light of 546 nm.

D. NMR data collection

MAS NMR spectra for the isostatically compressed samples were collected for ^{11}B, ^{23}Na, and ^{27}Al with a Varian Unity/Inova 600 spectrometer (14.1 T field) at 192.4, 158.6, and 156.3, MHz respectively, using a Varian/Chemagnetics probe, with 3.2 mm zirconia rotors, and spinning rates of 20 kHz. MAS spectra for ^{29}Si were collected with a Varian Infinity Plus 400 spectrometer (9.4 T) at 79.4 MHz with a similar probe at spinning rates of 12 kHz. Frequencies are referenced to 1.0M boric acid (19.6 ppm), 0.1M NaCl (0 ppm), 0.1M $Al(NO_3)_3$ (0 ppm), and tetramethylsilane (0 ppm). Single-pulse acquisition was used, with pulse lengths of 0.3, 0.2, 0.2, and 0.7 μs and radiofrequency (rf) fields of about 100, 125, 125, and 130 kHz for ^{11}B, ^{23}Na, ^{27}Al, and ^{29}Si respectively. Spectra for ^{27}Al were also acquired with a Varian 800 spectrometer (18.8 T), using a similar probe and experimental conditions. A small background signal was subtracted using data for the empty sample rotor. Spectra were fitted with the program "DMFIT", which simulates quadrupolar lineshapes with distributions of parameters such as chemical shift and quadrupolar coupling constants, and has often been used to analyze such spectra for aluminosilicate glasses.[31,32] No differential relaxation was observed for any of these nuclides with pulse delays ranging from 0.1 to 10 s, except for some broadening of ^{29}Si spectra at the shortest delays. The Fe content of the glass ensured relatively rapid spin-lattice relaxation.

For the static (non-MAS) spectra of the uniaxially compressed samples (142 MPa), a 3.5 mm cube was cut from the center of the deformed cylinder, oriented with one face perpendicular to the compression direction. This was attached to a plastic rod to allow rotation inside of the 5 mm diameter, horizontal solenoidal coil of a Varian "wideline" probe. Spectra were collected with a Varian Infinity 400 spectrometer (9.4 T) for ^{11}B, ^{23}Na, and ^{27}Al (128.3, 105.7, and 104.2 MHz) to enhance any effects of orientation on the second-order quadrupolar line shape; static ^{29}Si were also acquired at this field. Pulse lengths were 0.5 μs and radiofrequency (rf) fields were about 80, 60 and 60 kHz for ^{11}B, ^{23}Na, and ^{27}Al, respectively. For ^{29}Si, a spin-echo pulse sequence ($90-\tau-180$) was used to eliminate effects of deadtime, with 4 and 8 μs pulses. For each nuclide, several spectra were collected with orientations such that the compression direction was either perpendicular to the external magnetic field or parallel to it. In all cases, only the central transition ($\pm1/2$) peak was observed.

TABLE II. Birefringence data for uniaxially compressed E-glass.

Sample No.	P (MPa)	T (K)	Cooling rate (K min^{-1})	Thickness of platelet (mm)	Birefringence (nm mm^{-1})
EG/0.6 uni	0.5	966	5	3.563	1.20, 1.20, 1.38
EG/81 uni	81	966	5	3.566	13.54, 13.54, 14.12
EG/101 uni	101	966	5	3.588	15.59, 15.28, 14.08
EG/117 uni	117	966	5	3.576	17.43, 17.43, 18.09
EG/142 uni	142	966	5	3.562	20.64, 18.56, 20.99

III. RESULTS

A. Density and birefringence data

Measured densities are shown in Fig. 1. Recovered densities increase systematically and approximately linearly with the run pressure, reaching a maximum increase in 2.1% at 500 MPa. Applying linear regression to the data we calculated $\rho=2.6373\ \text{g cm}^{-3}+(1.08\times10^{-4}\ \text{g cm}^{-3}\ \text{MPa}^{-1})\times p$ for isostatically compressed E-glass (with p in MPa). For all samples, the measured refractive index was smaller parallel to the direction of compressive stress, and larger perpendicular to the compression direction, i.e., representing an indicatrix of oblate spheroidal shape (Table II). The optical character is similar to that of a uniaxially negative crystal. The negative birefringence was found to increase systematically with axial compressive stress reaching a maximum increase of $\Delta n/n=(-)12.9$ ppm at 150 MPa (Fig. 2). The optical character of the compressed cylinders was opposite to that of the previously studied E-glass fibers, where the indicatrix is represented by an prolate spheroid (optically positive crystal).[26,29] Based on the definition for compressive stresses $\sigma<0$ and tensile stresses $\sigma_t>0$ and assuming linear dependence of the data of Fig. 2 the value of $(+)0.149\pm0.003$ nm mm^{-1} MPa^{-1} was calculated for the specific birefringence $\Delta(\Delta n)/\Delta\sigma$ of uniaxially compressed E-glass. In accordance with other borosilicate glasses[5] the specific birefringence in E-glass samples is positive and seems to increase with decreasing viscosity (see insert of Fig. 2). It is lower for uniaxially compressed cylinders with $T_f\approx T_g$ and higher for hyperquenched fibers with $T_f>T_g$.

B. MAS NMR results

The ^{11}B MAS spectra (Fig. 3) show good resolution between the peaks for ^{III}B (centered at about 12 ppm) and for ^{IV}B (centered at about 0 ppm), as is typical at this field.[33] Integrated peak areas, corrected for the overlapped central spinning sidebands of the satellite transitions, were used to calculate "N_4," the ratio of tetrahedral to total boron. This parameter, and thus the mean coordination number of the boron cations, increases substantially and systematically with pressure from 0.230 to 0.285 (Fig. 1).

The ^{27}Al MAS spectra (Fig. 4) are dominated by an asymmetrical peak, centered at 57 ppm (18.8 T), that is typical of ^{IV}Al in aluminoborosilicate glasses.[33] At about 30 and 0 ppm are partially resolved shoulders that correspond to small concentrations of ^{V}Al and ^{VI}Al.[31,33,34] Comparison of spectra clearly shows that both of the higher-coordinated species increase in relative abundance with increasing pressure. Fitted peak shapes yield estimates of their concentrations (Table III) that range from about $4.4\pm0.5\%$ and $0.5\pm0.2\%$ of total Al for ^{V}Al and ^{VI}Al respectively in the ambient pressure sample to $6.9\pm0.5\%$ and $1.2\pm0.5\%$ in the

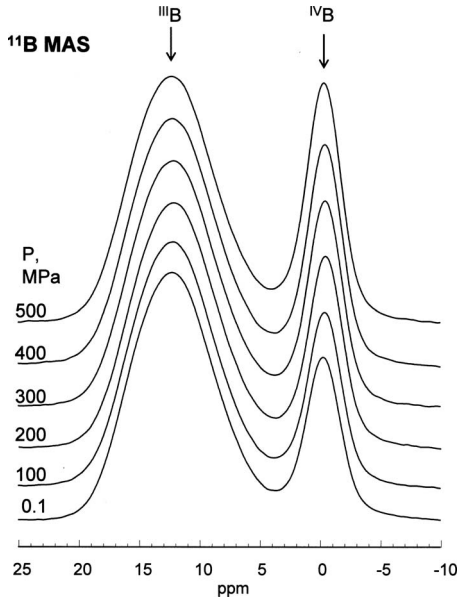

FIG. 3. ^{11}B MAS NMR spectra for isostatically compressed E-glass samples (14.1 T), normalized to height of ^{III}B peak.

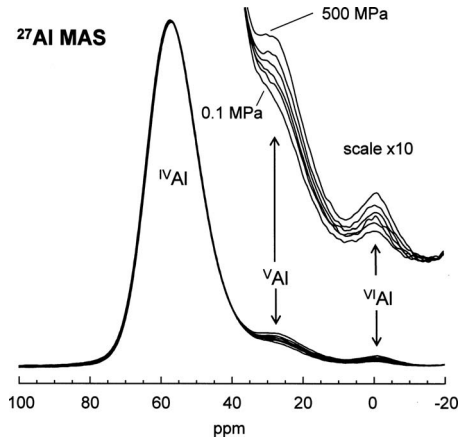

FIG. 4. ^{27}Al MAS NMR spectra for isostatically compressed E-glass samples (18.8 T), normalized to height of ^{IV}Al peak. Spectra are overlaid to highlight increases in ^{V}Al and ^{VI}Al with pressure, which increases progressively from lowest (0.1 MPa) to uppermost (500 MPa) curve. The inset has vertical scale $\times$ 10.

TABLE III. Run conditions, density, and structural data for isostatically compressed E-glass.

Sample No.	P (MPa)	T (K)	Cooling rate (K min^{-1})	Density (g cm^{-3})	N_4	^{V}Al	^{VI}Al
EG/0.1 iso	0.1	978	4.0	2.6365	0.230	0.044	0.005
EG/100 iso	100	988	4.4	2.6497	0.247	0.050	0.006
EG/200 iso	200	983	4.4	2.6596	0.256	0.053	0.007
EG/300 iso	300	983	4.5	2.6686	0.260	0.058	0.008
EG/400 iso	400	988	4.5	2.6791	0.265	0.062	0.009
EG/500 iso	500	987	4.4	2.6929	0.288	0.069	0.012

Notes:
N_4 is fraction of total B present as ^{IV}B; ^{V}Al and ^{VI}Al are fractions of total Al.

500 MPa glass, in the range expected from previous NMR studies of ambient pressure an E-glass sample of similar but not identical composition.[33]

As is typical for all oxide glasses, ^{23}Na MAS spectra (Fig. 5) are unresolved into components for different coordination numbers or types of neighbors (e.g., BO versus NBO), although distributions in both are likely to be present.[35] However, peak positions do shift systematically with pressure, moving slightly to higher frequency. Because at these high fields, ^{23}Na MAS NMR peaks are largely controlled by distributions of chemical shifts (δ_{iso}), and to a lesser extent by second-order quadrupolar broadening, this shift with pressure is most likely the result of a decrease in the mean Na–O bond distance, which is correlated with δ_{iso}, having a slope of roughly –0.0015 nm ppm^{-1} based on data for crystalline silicates.[36–38] In previous studies of aluminosilicate glasses, this effect was confirmed by comparing peak positions and widths at 14.1 and 18.8 T and calculating the mean δ_{iso} for the ambient pressure and high-pressure glasses[23,24,34] or for aluminoborosilicates with varying Na/Ca ratios.[39] For the data presented here, an increase in δ_{iso} of 1.5 ppm suggests a decrease in mean Na–O by about 2 pm from ambient pressure to 500 MPa, or a shortening of about 0.7%.

Figure 6 shows ^{29}Si MAS spectra for the ambient pressure and 500 MPa glasses. Again as is typical for aluminosilicates and borosilicates, there is no resolution among signals for different Si species, either with varying numbers of BO/NBO or of Al, B, and Si neighbors:[33] The disorder in the structure simply overwhelms the differences in chemical shifts. Analysis of these spectra would thus be highly model dependent. However, it is clear that there is a systematic shift with increasing pressure toward higher (less negative) chemical shifts. In simpler alkali silicate and alkali aluminosilicate glasses formed at high pressure, this type of change has also been observed and was suggested to be related to reductions in mean Si–O–(Si,Al) bond angles,[23,40] which are known to be correlated with chemical shift.[41] Although this interpretation of the results on E-glass is not unique, it seems plausible for these samples.

C. Static NMR results

As shown in Fig. 7, the static spectra for ^{11}B, ^{23}Na, ^{27}Al, and ^{29}Si are all unresolved into components for differing structural species, as is typical for glasses at 9.4 T. The full widths at half maxima are about 8, 10, 12, and 5 kHz, respectively. The peak for ^{11}B is made somewhat asymmetric by the overlap of the relatively broad signal from the predominant ^{III}B sites, which have quadrupolar coupling constants (C_Q) of about 2.5–3 MHz, with the relatively narrow component for the ^{IV}B sites, which have much smaller C_Q values.[15,41] Although we have not attempted to simulate these line shapes, their widths for the three quadrupolar nuclides (^{11}B, ^{23}Na, and ^{27}Al) are probably dominated by quadrupolar

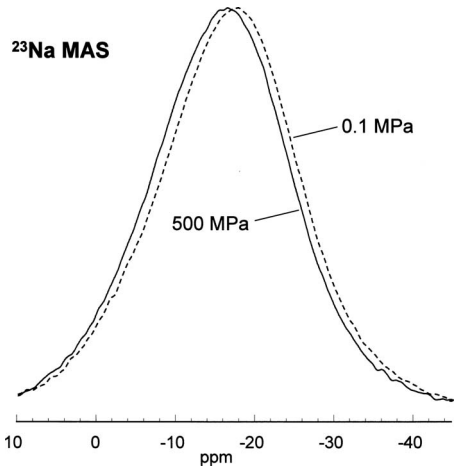

FIG. 5. ^{23}Na MAS spectra for isostatically compressed E-glass samples (14.1 T). Data only for 0.1 MPa (dashed line) and 500 MPa (solid line) are plotted for clarity; 300 MPa glass spectrum would plot between these two curves.

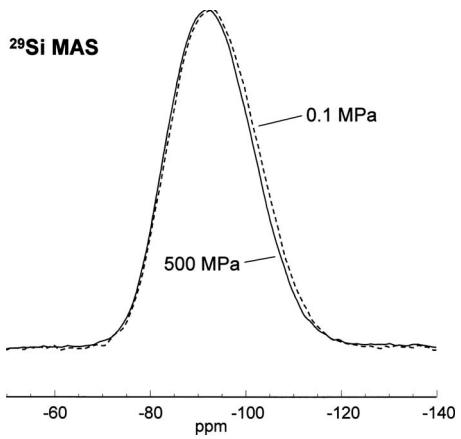

FIG. 6. ^{29}Si MAS spectra for isostatically compressed E-glass samples (9.4 T). Data only for 0.1 MPa (dashed line) and 500 MPa (solid line) are plotted for clarity.

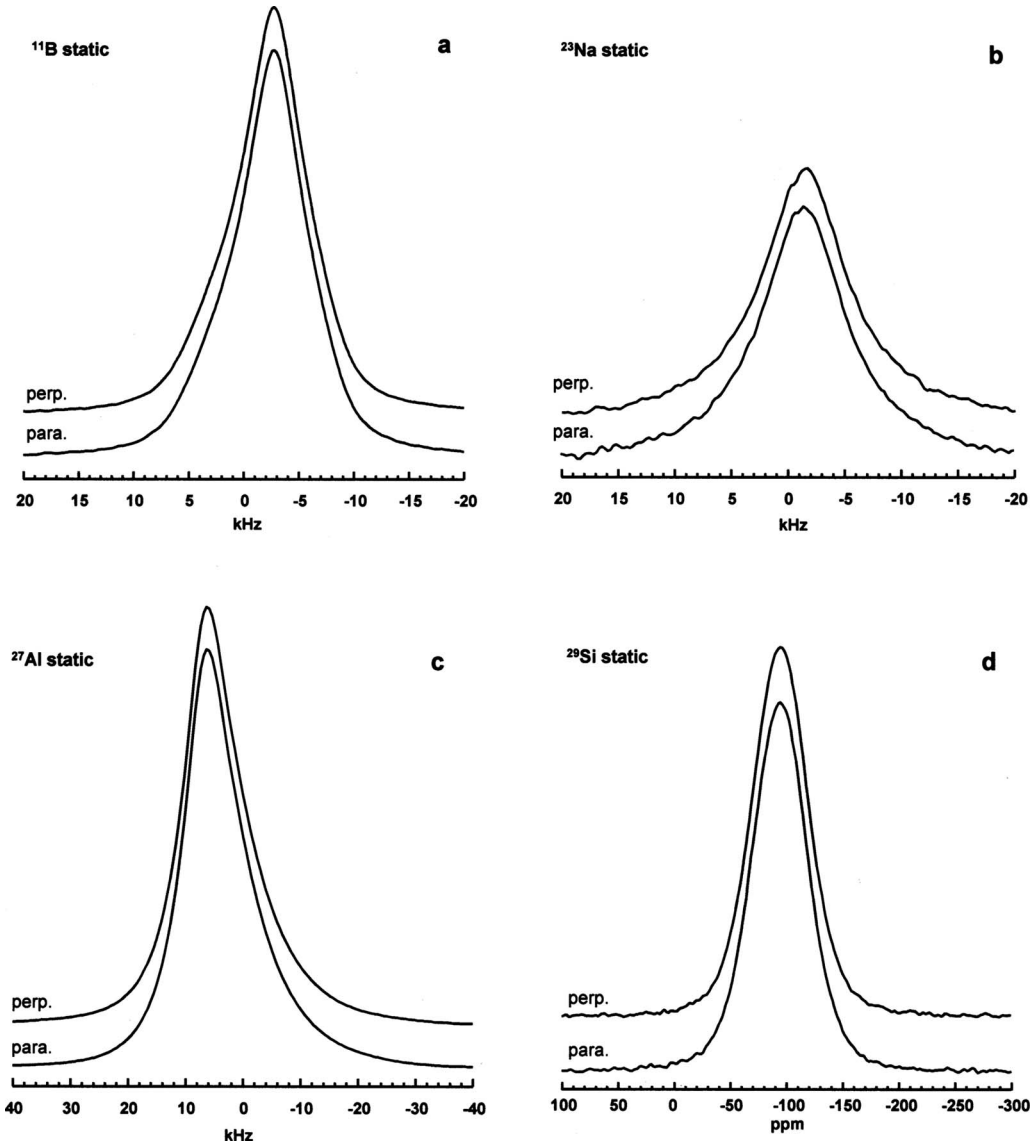

FIG. 7. Static spectra on cubes of uniaxially compressed E-glass (142 MPa, 9.4 T), with the orientation of the compression direction relative to the external magnetic field as labeled. (a) ^{11}B; (b) ^{23}Na; (c) ^{27}Al; (d) ^{29}Si.

broadening, and by distributions in quadrupolar parameters and chemical shifts. The widths are consistent with the static quadrupolar line widths (central transitions) expected for typical C_Q values of 2.5–3 MHz for ^{11}B,[3] 2–3 MHz for ^{23}Na,[35] and 4–6 MHz for ^{27}Al,[42] with considerable smoothing out of the quadrupolar line shapes by the distributions in NMR parameters caused by the disordered glass structure. Homo- or heteronuclear dipolar broadening from these three nuclides (the only ones present that have isotopic abundances and resonant frequencies high enough to potentially cause significant dipolar coupling) will probably have lesser effects on line widths for ^{11}B and ^{27}Al:Na is chemically low in abundance, and most B and Al probably have mostly Si first cation neighbors because of the relatively high Si/Al and Si/B ratios. On the other hand, it is likely that most Na^+ cations are near to Al or B in their role as charge compensators for partially charged bridging oxygens such as Si–O–^{IV}Al and Si–O–^{IV}B, and thus may experience more important dipolar broadening. The line shape for the static ^{29}Si spectra is probably affected both by dipolar couplings and chemical shift anisotropy.

There is no detectable effect of orientation on the static NMR spectra for ^{11}B of the E-glass sample that was deformed under uniaxial stress [Fig. 7(a)]. Because trigonal BO_3 groups have local electric field gradients that are highly asymmetrical, because these are the predominant boron species in this composition, and because the second-order quadrupolar coupling has a significant influence on the static ^{III}B line shape at this field, it can be shown that even small variations from random orientation (e.g., several percent of the ^{III}B groups aligned during flow) would lead to measurable changes in the peak shape.[10] It can thus be concluded that if there is alignment of these highly anisotropic structural units during flow (which we do not know), then most or all of this relaxes back to a random distribution before the structure finally "freezes" at the glass transition, as was previously concluded for a variety of borate and silicate glasses that

TABLE IV. Comparison of effects of pressure on speciation in several glass compositions. Data for maximum pressures only are shown; see Table I for compositions.

Glass	p (MPa)	N_4	NBO[a]	$d\ln(K)/dp$ [b] (MPa^{-1})	$d\ln(K')/dp$ [c] (MPa^{-1})
E-glass (this study)	0.1	0.230	0.175	0.65×10^{-3}	0.61×10^{-3}
	500	0.288	0.172		
Na-borosilicate[d]	0.1	0.893	0.073	1.48×10^{-3}	1.33×10^{-3}
	500	0.942	0.068		
Na-borosilicate[e]	0.1	0.62	0.11	0.40×10^{-3}	0.25×10^{-3}
	5000	0.85	0.052		

[a]Estimated from composition as described in text.
[b]Pressure derivative of apparent equilibrium constant, including NBO [Eq. (2)].
[c]Pressure derivative of apparent equilibrium constant, not including NBO [Eq. (3)].
[d]Reference 17.
[e]Reference 15.

were strained during quenching, including fast-quenched E-glass fibers.[10] Of course, it is also possible that such preferred orientation does not occur in the deforming melt, given the complexities of the way that stress can be transferred through a complex network structure and the importance of local bond breaking in controlling the flow in such materials.[10]

For the static ^{23}Na, ^{27}Al, and ^{29}Si spectra, there are also no hints of orientational effects [Figs. 7(b)–7(d)]. The bonding environments of these cations should be more symmetrical than those of BO_3 groups. A cation with relatively weak ionic bonds and a relatively high coordination number such as Na^+ probably has a roughly spherical environment. The more strongly bonded Al^{3+} cation is expected to be primarily in tetrahedral sites with four bridging oxygens and mostly Si neighbors,[19,43] again giving a relatively symmetrical local structure. These structural units might therefore be less likely to align during flow because of their relative lack of bonding anisotropy when compared to ^{III}B. However, if the whole glass was strained enough to compress or stretch Al–O or Na–O bonds significantly in ways that correlate with the compression direction, then an effect on the static NMR line shapes would be expected if the electric field gradient tensors developed sufficient preferential orientation. Most Si will be in sites with four bridging oxygens ("Q^4"), with mostly Si but also B and Al neighbors. Some Si sites with one or more NBO will also be present, but these are in the minority. For at least the Q^4 sites, local alignment during flow, in the sense of nonrandom distribution of bond directions, would again probably not be expected. However once more, deformation of the glass could, in principle, create nonrandom orientations to the chemical shift anisotropy for ^{29}Si that could affect the NMR spectra. However, the sensitivity of any of these effects to a given degree of deformation is not simply quantified.

IV. DISCUSSION

A. Pressure effects on structure in different glass compositions

In a recent study of a sodium borosilicate glass compressed at pressures to 500 MPa in experiments similar to those described here,[17] recovered density increases of up to 2.3% were observed, which are similar to those described here for E-glass. In the previous study, ^{11}B MAS NMR also showed roughly comparable increments in the fraction of ^{IV}B, denoted here as N_4 (a maximum increase in about 0.05 versus 0.06 here), although the absolute N_4 values were much higher for that composition (ranging from 0.89 to 0.94).

Based, in part, on long-studied effects of temperature on speciation in borate glasses,[12–14,17,33,44,45] it has been proposed that one mechanism of converting ^{III}B to ^{IV}B can be written as

$$BO_3 + NBO = BO_4 \quad (1)$$

although it should be noted that this form is somewhat incomplete as it does not describe accompanying changes in modifier cations or in network connectivity.[46] The role of this mechanism was confirmed in a recent ^{11}B and ^{17}O NMR study of a different sodium borosilicate glass quenched from a melt at 5 GPa, in which boron and oxygen speciation were independently measured and found to change as predicted (Table IV).[15] It can be useful to express changes with temperature or pressure in a thermodynamic form, such that an idealized apparent equilibrium constant can be calculated from the molar concentrations simply as[13,14]

$$K = {}^{IV}B/({}^{III}B \times NBO). \quad (2)$$

If the NBO content stays roughly constant (i.e., changes in boron speciation are small), then a further approximation can be made:[17]

$$K' = {}^{IV}B/{}^{III}B. \quad (3)$$

With either formulation, the change in $\ln(K)$ with pressure could be related to the volume change associated with reaction (1),[17] and can thus serve as a useful means of comparing different data sets. A similar approach was taken for the transition from ^{IV}Al to ^{V}Al and ^{VI}Al with pressure in aluminosilicate glasses.[21]

Lacking direct measurements by ^{17}O NMR or other approaches, NBO contents can readily be estimated from glass composition and measured N_4 values.[15,22] This generally requires assumptions that there are no oxygens coordinated by

three network cations ("triclusters"), that ^{V}Al and ^{VI}Al are minor species and can either be ignored (as will be done here), or corrected for, and that all oxygens are bonded to one or two network cations (i.e., no "free oxide ions"). For the composition studied by Wondraczek *et al.*,[17] the calculated NBO content of the ambient pressure glass is 7.3% of total oxygens; for the E-glass described here (further ignoring the F content) we obtain 17.5% at ambient pressure. For the Na borosilicate described in the study to 5 GPa,[15] the value is 11%.

The effect of pressure on either K or on K' varies somewhat among the three compositions, when expressed as $d\ln(K)/dp$ or $d\ln(K')/dp$ (Table IV). The apparent pressure effect is several times higher in the 500 MPa sodium borosilicate experiments than for the E-glass, which in turn is several times higher than for the 5 GPa sodium borosilicate. Given that the first two sets of samples were prepared with similar methods and p/T conditions, it is likely that this difference is an effect of composition. In particular, the replacement of the network modifier oxide Na_2O by CaO in borosilicate and aluminoborosilicates is known to have a large effect on increasing NBO content and thus decreasing N_4, as noted above for these two compositions at ambient pressure.[39] This is thought to result from the stabilization of NBO (and thus the displacement of reaction (1) to the left for same thermal history) by the much higher cation field strength of Ca^{2+} vs. Na^{+}. A similar effect might result in a reduced transformation rate with increasing pressure, although we note that for aluminosilicates, higher modifier cation field strength generally *increases* the amount of Al coordination increase with pressure.[21,24] In thermodynamic terms, the activity coefficient for the NBO (and for the boron species), which is ignored in these formulations, may thus depend strongly on composition, leading to different variation with pressure. Considering the high-pressure experiments performed by Du *et al.*,[15] one may further note that their samples experienced relatively fast quench rates. Therefore, the opposite effects of T_f and p_f on N_4 as well as density are superimposed in this case. Further differences in the observed pressure effects could be a result of compositional differences (e.g., the very different B/Si ratios) and possible nonlinear effects of pressure on $\ln(K)$ or activities.

B. Relationship of structural changes to density changes

An important and obvious question is how large a role is played by observed changes in cation coordination with pressure in the overall densification of a glass. A simple approach to this problem is to consider the effects of partial molar volumes of the oxide components of the bulk composition. This method is, for example, well developed for parametrizing the molar volumes of multicomponent silicate liquids at ambient pressure, which are defined as the sums of the products of oxide mole fractions and partial molar volumes V_i, with the latter approximated as independent of composition.[47]

For the E-glass data described here, one limiting scenario could be that most or all of the observed densification is governed by conversion of ^{III}B to ^{IV}B,[45] and thus can be accounted for by a difference in V_i for B_2O_3 with three-coordinated boron (V_{III}) and V_i for B_2O_3 with four-coordinated boron (V_{IV}). An extreme (and rather unlikely) minimum ratio V_{IV}/V_{III} could be taken as 0.5. That this is an extreme value can be seen from the ratio of the molar volumes of diamond (^{IV}C) to graphite (^{III}C) of 0.64, and of the ratio of the molar volume of α-alumina ($^{VI}Al_2O_3$) to V_i for the $^{IV}Al_2O_3$ component in aluminosilicate melts (0.68), or of that of stishovite ($^{VI}SiO_2$) to V_i for the $^{IV}SiO_2$ component of melts (0.52).[23,47] V_{III} can be approximated as that for pure B_2O_3 glass (38.4 cm^3/mol,[48] possibly an overestimate given the open ring structure of the pure glass, which may not be present in aluminosilicates); thus V_{IV} would be 19.2 $cm^3\ mol^{-1}$. The sum of V_i for all other components (V_{rest}) is then calculated from the ambient pressure density and the gram formula weight (which yield the overall molar volume of 24.0 $cm^3\ mol^{-1}$) and the measured boron speciation, giving $V_{rest}=23.4\ cm^3\ mol^{-1}$. This calculation simply takes V_{rest} as a constant, and does not require modeling the individual oxide component volumes other than of B_2O_3. Keeping V_{rest} constant but adjusting the boron speciation to the observed 500 MPa values, a change in volume of only 0.3% is predicted, much smaller than the observed density increase of 2.1%. It thus seems unlikely that the overall density change of the glass can be simply attributed to an increase in the boron coordination: In effect, there is simply not enough boron in the glass for its coordination to dominate density changes. The same conclusion would be reached for any reasonable assumption about V_{III} (smaller values compound the discrepancy) and for even smaller ratios of V_{IV}/V_{III}: In fact, physically meaningless negative values for V_{IV} are obtained if the problem is inverted. A similar conclusion would be reached from observed changes in Al coordination with pressure in the E-glass. In recent studies of Al and Si coordination changes in high-pressure aluminosilicate glasses, it was also found by similar reasoning that the density changes that could be directly attributed to network cation coordination increase were at most a minor part of the overall densification.[23,34]

A more complete description must thus involve other important structural changes that take place during compression, such as the compaction of "soft" cation sites, network bond angle reduction, and perhaps changes in network ring statistics.[19] The observed boron and aluminum coordination increases are thus only part of the overall response of the network, although they may facilitate changes that would not take place in the absence of coordination shifts, such as the loss of nonbridging oxygens. If, instead of the scenario discussed above, all components of the glass including B_2O_3 are compacted equally, with the observed change in boron speciation the values of V_{III} and V_{IV} must be consistent with the 2.1% densification of the E-glass through the equality:

$$(1-N_{4,0})V_{III}+N_{4,0}V_{IV} = 1.021\times[(1-N_{4,500})V_{III}+N_{4,500}V_{IV}], \quad (4)$$

where the subscripts on N_4 denote pressure. This equation can be rearranged to yield the ratio $V_{IV}/V_{III}=0.67$, indepen-

dent of the assumed value of V_{III}. From the previously reported data on a sodium borosilicate glass,[17] the same calculation gives a similar value of $V_{IV}/V_{III}=0.67$ for the 500 MPa densification of 2.3%. This approach is somewhat oversimplified because other changes in the network, e.g., network bond angle compression, will affect the volumetric contributions from all network components, including boron. In turn, the large changes in boron coordination alter the fractions and distributions of bridging and nonbridging oxygens, and the network cation connectivity. These in turn change the modifier cation environments. All of these changes may affect properties, including density, in complex ways that make borosilicates especially sensitive to effects of both pressure and temperature. This sensitivity can also be assessed by the difference of approximately 1% in the increase of density per 500 MPa pressure between boron-bearing glasses (2.1%, Table II) and boron-free silicate glasses (0.8%–1.2%).[18]

In several recent studies of high-pressure sodium aluminosilicate glasses, increases in ^{23}Na chemical shifts with synthesis pressure have suggested small reductions in mean Na–O bond distances.[20,23,24,34] The 0.7% reduction in this distance estimated from the data presented above for the 500 MPa E-glass would correspond to a reduction in volume of the Na–O coordination sphere of $1.007^3=1.021$, or a 2.1% compaction, which is surprisingly similar to the overall density increase of the sample. Although Na is only a small component of the glass, perhaps it serves as a useful probe of the overall degree of compaction in these samples. It is noteworthy that this observation is confirmed by previous comparative studies of the recovered density increases in a borosilicate and boron-free alkali silicate glasses:[18] Regardless of short-range structural changes in N_4, in the pressure regime considered, macroscopic compaction is roughly similar in these glasses. It was thus argued that changes in molar volume are predominantly governed by midrange effects and/or the packing density of short-range structural elements (such as Na–O coordination spheres). In contrast, short-range structural changes are reflected by a strong dependence of potential energy (excess enthalpy) on pressure. In borosilicate glasses, the observed parallelism of the relaxation functions for molar volume and for short-range structure (concentration of N_4, Prigogine–Defay ratio close to unity) then indicates dominance of a single structural parameter in the glass transition. On the other hand, in boron-free silicate glasses, the structural origin of relaxation is more complex in that more parameters play equally important roles. In that case, caloric and mechanical relaxation functions are decoupled to a larger extent.

C. Birefringence and flow

There is very little direct structural evidence for the source of birefringence in borosilicate glasses that have been deformed during quench, such as the uniaxially compressed samples described here. In one previous study, ^{11}B and ^{29}Si NMR of several types of borosilicate and silicate sheets and fibers (including 6 μm E-glass fibers) showed no effects of orientation, even for structural groups that have large local anisotropies, e.g., ^{III}B and Si in Q^3 sites with three bridging oxygen neighbors.[10] There it was suggested that this negative finding results from the similarity of the time scales of network bond breaking and rearrangement and the shear relaxation time near to T_g, allowing relaxation of small-scale anisotropy as long as deformation is occurring. This conclusion was related to direct, high-temperature NMR measurements of the local structural exchange rates in several silicate and borate liquids.[49,50] In contrast, a ^{31}P NMR study of extruded rods of a calcium metaphosphate glass did indicate that some nonrandom orientation of the phosphate units was retained on cooling through T_g, perhaps suggesting a more polymer-like behavior.[7,8] Birefringence is well known in deformed glasses, especially in fibers (see Sec. I), and was reported in both of the previous NMR studies of anisotropy.

As described above, the uniaxially compressed E-glass samples also have readily measurable birefringence, but lack local structural anisotropy that is detectable by NMR. One possible explanation of this observation was suggested previously,[10] that intermediate-scale compositional or structural heterogeneities,[51,52] or other sources of local density fluctuations, become deformed during flow. If such heterogeneities are considerably larger than the local structural units sampled by NMR (but smaller than optical wavelengths, of course), their homogenization could require diffusion times that are much longer than the shear relaxation time, and therefore they persist on quenching. Heterogeneities with regard to subcritical clusters of crystalline phases (intermediate range structure) were suggested to affect the optical birefringence in alkali silicate glasses with reduced glass transition temperature $T_{rg}<0.6$ ($T_{rg}=T_g/T_{\text{liquidus}}$).[53] In these glasses an anomalous birefringence was observed,[54] which increased with decreasing T_{rg}. (Decreasing T_{rg} values were correlated with increasing nucleation tendency, i.e., increasing maximum nucleation rates in silicate glasses.[55])

However, a recent study of annealing effects on E-glass fibers showed that birefringence relaxed considerably faster than the bulk enthalpy.[26] Given that the latter is largely controlled by configurational rearrangements that often require breaking and reforming of energetic network bonds,[29,45] this finding suggests that birefringence may be primarily related to local, small-scale anisotropic stretching or compression of bond distances or angles, probably accompanied by deformation of the coordination shells of modifier cations, that are energetically less difficult to restore to isotropy because they require only small local displacement of ions. The large energetic difference between anisotropy relaxation (fast) and network relaxation (slow) in E-glass fibers was quantified recently by a low coupling ratio of 0.06, which was close to that of alkali mobility from network relaxation.[29] However, the distortions causing birefringence must be large enough to measurably perturb the refractive index (ppm in refractive index differences), but apparently in the samples studied here are not sufficient to result in effects on static NMR spectra. Future theoretical calculations on the consequences of such distortions, for example the deformation of modifier cation environments by anisotropic compression of network cages, could lead to predictions of effects on electric field gradients and/or chemical shift anisotropy that could help to quantify this problem.

ACKNOWLEDGMENTS

J.D. and L.G. thank the Deutsche Forschungsgemeinschaft (DFG) for financial support (Grant No. DE598/8-1). J.W. and J.F.S. acknowledge the support of the U.S. National Science Foundation, Grant No. DMR 0404972. L.W. thanks the DFG for further financial support under Grant No. WO1220/3-1. We thank N. Kim for assistance with XRD and D. Massiot (CNRS, Orléans, France) for making the "DMFIT" software freely available.

[1] R. Brückner and A. Habeck, Glastech. Ber. Glass Sci. Technol. **67**, 1 (1994).
[2] R. Brückner, Glastech. Ber. Glass Sci. Technol. **67C**, 161 (1994).
[3] T. Takamori and M. Tomozawa, in *Treatise on Materials Science and Technology*, Glass I: Interaction with Electromagnetic Radiation Vol. 12, edited by M. Tomozawa and R. H. Doremus (Academic, New York, 1977), pp. 123–155.
[4] B. Martin, Y. Yue, L. Wondraczek, and J. Deubener, Appl. Phys. Lett. **86**, 121917 (2005).
[5] R. Brückner, Glastech. Ber. Glass Sci. Technol. **69**, 396 (1996).
[6] A. Habeck and R. Brückner, J. Non-Cryst. Solids **162**, 225 (1993).
[7] M. Braun, Y. Yue, C. Rüssel, and C. Jäger, J. Non-Cryst. Solids **241**, 204 (1998).
[8] Y. Z. Yue, M. Braun, C. Rüssel, G. Carl, and C. Jäger, Phys. Chem. Glasses **41**, 12 (2000).
[9] H. Stockhorst and R. Brückner, J. Non-Cryst. Solids **85**, 105 (1986).
[10] J. F. Stebbins, D. R. Spearing, and I. Farnan, J. Non-Cryst. Solids **110**, 1 (1989).
[11] P. J. Bray and E. J. Holupka, J. Non-Cryst. Solids **71**, 411 (1985).
[12] P. K. Gupta, M. L. Lui, and P. J. Bray, J. Am. Ceram. Soc. **68**, C-82 (1985).
[13] J. F. Stebbins and S. E. Ellsworth, J. Am. Ceram. Soc. **79**, 2247 (1996).
[14] S. Sen, Z. Xu, and J. F. Stebbins, J. Non-Cryst. Solids **226**, 29 (1998).
[15] L. S. Du, J. R. Allwardt, B. C. Schmidt, and J. F. Stebbins, J. Non-Cryst. Solids **337**, 196 (2004).
[16] S. K. Lee, K. Mibe, Y. W. Fei, G. D. Cody, and B. O. Mysen, Phys. Rev. Lett. **94**, 165507 (2005).
[17] L. Wondraczek, S. Sen, H. Behrens, and R. E. Youngman, Phys. Rev. B **76**, 014202 (2007).
[18] L. Wondraczek and H. Behrens, J. Chem. Phys. **127**, 154503 (2007).
[19] B. O. Mysen and P. Richet, *Silicate Glasses and Melts, Properties and Structure* (Elsevier, Amsterdam, 2005).
[20] S. K. Lee, G. D. Cody, Y. Fei, and B. O. Mysen, Chem. Geol. **229**, 162 (2006).
[21] J. A. Allwardt, J. F. Stebbins, H. Terasaki, L.-S. Du, D. J. Frost, A. C. Withers, M. M. Hirschmann, A. Susuki, and E. Ohtani, Am. Mineral. **92**, 1093 (2007).
[22] L.-S. Du and J. F. Stebbins, J. Non-Cryst. Solids **351**, 3508 (2005).
[23] K. E. Kelsey, J. F. Stebbins, J. L. Mosenfelder, and P. D. Asimov, Am. Mineral. **94**, 1205 (2009).
[24] K. E. Kelsey, J. F. Stebbins, D. M. Singer, G. E. Jr, and J. L. Brown, Geochim. Cosmochim. Acta **73**, 3914 (2009).
[25] D. L. Farber and Q. Williams, Am. Mineral. **81**, 273 (1996).
[26] M. Ya, J. Deubener, and Y. Yue, J. Am. Ceram. Soc. **91**, 745 (2008).
[27] G. Pähler and R. Brückner, Glastech. Ber. **54**, 52 (1981).
[28] H. Stockhorst and R. Brückner, J. Non-Cryst. Solids **49**, 471 (1982).
[29] J. Deubener, Y. Z. Yue, H. Bornhöft, and M. Ya, Chem. Geol. **256**, 299 (2008).
[30] L. Wondraczek, H. Behrens, Y. Yue, J. Deubener, and G. W. Scherer, J. Am. Ceram. Soc. **90**, 1556 (2007).
[31] D. R. Neuville, L. Cormier, and D. Massiot, Geochim. Cosmochim. Acta **68**, 5071 (2004).
[32] D. Massiot, F. Fayon, M. Capron, I. King, S. L. Calvé, B. Alonso, J. O. Durand, B. Bujoli, Z. Gan, and G. Hoatson, Magn. Reson. Chem. **68**, 5071 (2002).
[33] T. J. Kiczenski, L. S. Du, and J. Stebbins, J. Non-Cryst. Solids **351**, 3571 (2005).
[34] J. R. Allwardt, J. F. Stebbins, B. C. Schmidt, D. J. Frost, A. C. Withers, and M. M. Hirschmann, Am. Mineral. **90**, 1218 (2005).
[35] S. K. Lee and J. F. Stebbins, Geochim. Cosmochim. Acta **67**, 1699 (2003).
[36] X. Xue and J. F. Stebbins, Phys. Chem. Miner. **20**, 297 (1993). ^{23}Na
[37] A. M. George, S. Sen, and J. F. Stebbins, Solid State Nucl. Magn. Reson. **10**, 9 (1997).
[38] J. F. Stebbins, Solid State Ionics **112**, 137 (1998).
[39] J. Wu and J. F. Stebbins, J. Non-Cryst. Solids **355**, 556 (2009).
[40] X. Xue, J. F. Stebbins, M. Kanzaki, P. F. McMillan, and B. Poe, Am. Mineral. **76**, 8 (1991).
[41] K. J. D. MacKenzie and M. E. Smith, *Multinuclear Solid-State NMR of Inorganic Materials* (Pergamon, New York, 2002).
[42] D. R. Neuville, L. Cormier, and D. Massiot, Chem. Geol. **229**, 173 (2006).
[43] J. R. Allwardt, S. K. Lee, and J. F. Stebbins, Am. Mineral. **88**, 949 (2003).
[44] R. J. Araujo, Phys. Chem. Glasses **21**, 193 (1980).
[45] S. Sen, T. Topping, P. Yu, and R. E. Youngman, Phys. Rev. B **75**, 094203 (2007).
[46] J. F. Stebbins, E. V. Dubinsky, K. Kanehashi, and K. E. Kelsey, Geochim. Cosmochim. Acta **72**, 910 (2008).
[47] R. A. Lange, Contrib. Mineral. Petrol. **130**, 1 (1997).
[48] K. Budhwani and S. Feller, Phys. Chem. Glasses **36**, 183 (1995).
[49] I. Farnan and J. F. Stebbins, Science **265**, 1206 (1994).
[50] J. F. Stebbins and S. Sen, J. Non-Cryst. Solids **224**, 80 (1998).
[51] Y. Z. Yue, J. Non-Cryst. Solids **345–346**, 523 (2004).
[52] Y. Z. Yue, Ceram. Transact. **170**, 31 (2004).
[53] J. Deubener, J. Non-Cryst. Solids **351**, 1500 (2005).
[54] J. Deubener, F. de Moraes, and R. Brückner, J. Non-Cryst. Solids **219**, 57 (1997).
[55] J. Deubener, J. Non-Cryst. Solids **274**, 195 (2000).